Human-Robot Interaction Through Fingertip Haptic Devices for Cooperative Manipulation Tasks

Selma Musić[1], Domenico Prattichizzo[2], Sandra Hirche[1]

***Abstract*— Teleoperation of multi-robot systems, e.g. dual manipulators, in cooperative manipulation tasks requires haptic feedback of multi-contact interaction forces. Classical haptic devices restrict the workspace of the human operator and provide only one contact point. An alternative solution is to enable the operator to command the robot system via free-hand motions which extends the workspace of the human. In such a setting, a multi-contact haptic feedback may be provided to the human through multiple wearable haptic devices, e.g. fingertip devices that display forces on the human fingertips. In this paper we evaluate the benefit of using wearable haptic fingertip devices to interact with a bimanual robot setup in a pick-and-place manipulation task. We show that haptic feedback through wearable devices improves task performance compared to the base condition of no haptic feedback. Therefore, wearable haptic devices are a promising interface for guidance of multi-robot manipulation systems.**

I. INTRODUCTION

Haptic human-robot interaction is achieved through the exchange of forces between the human operator and a robot system. It can be in the form of a *direct physical interaction (pHRI)* [1] or *haptic device interaction*, e.g. in teleoperation or virtual environment settings [2]. Force feedback obtained through a haptic device is essential in tasks where the robot, guided by the operator, physically interacts with an unknown environment.

Haptic devices can be classified into *kinesthetic* and *cutaneous* haptic devices. Typical examples of kinesthetic haptic devices are *robot arms* [3], *table-top* devices [4], and *exoskeletons* [5]. Robot arms restrict the workspace of the operator to the workspace determined by the kinematic structure of the robot. Exoskeletons are wearable and, therefore, provide a larger workspace to the operator. However, both types of haptic devices can be heavy and the operator needs to apply additional effort to overcome their inertia. Table-top haptic devices are more compact and lighter, but restrict the workspace of the operator to his/her forearm workspace only. Cutaneous haptic devices are wearable, compact, light-weight, and have a relatively simple mechanical structure [6]. In consequence, they are not as precise as kinesthetic devices. However, while with kinesthetic devices a stability of the overall system may be an issue in the case of communication delays and stiff contacts, cutaneous haptic devices are intrinsically stable [7].

Kinesthetic haptic devices are typically coupled to the human hand through a single contact point. Therefore, multi-contact robot-environment interaction cannot be conveyed to the operator, e.g. in cooperative manipulation tasks [8]. Furthermore, as mentioned above, their workspace is often considerably smaller and different compared to the workspace of the robot, especially if the robot system is complex and/or mobile, e.g multi-manipulators, UAV(s), manipulators with mobile platforms, etc.

A possible solution may be to employ multiple *wearable cutaneous* haptic devices. For example, *fingertip cutaneous devices* are able to provide feedback about contact forces at the operator's fingertips [9]. They contain movable parts that exert pressure on the human skin, conveying in that way force information. Additionally, due to their wearability property, the workspace of the human operator is not restricted.

The suitability of wearable fingertip devices has been confirmed in a peg-in-hole task where the human teleoperates a robotic hand [7]. Furthermore, in [10] they are used to display object-curvature discrimination. Unlike previous work, we are interested in settings where the teleoperated system is not kinematically similar to the operator, i.e. we would like to investigate if these haptic devices are suitable for teleoperation of relatively large objects by robot manipulators.

In this paper, we evaluate the suitability of wearable thimble devices as haptic interfaces in a teleoperation of a dual-manipulator system cooperatively manipulating an object. We extend our previous work in which we propose a novel control architecture and conduct a within-subject analysis to evaluate the suitability of wearable haptics in this type of human-robot interaction [11]. In this work, a between-subject analysis is conducted to compare the task performance for multiple feedback types. The results further confirm the benefits of wearable haptic display in the interaction between a human operator and kinematically distinct robot system.

The paper is outlined as follows. In Section II we summarize the theoretical background and the used control approach. The experimental setup and the results of the user study are provided in Section III. Discussion of the results and conclusive remarks are given in Section IV and Section V, respectively.

II. THEORETICAL BACKGROUND

In this section we describe the control of the dual-manipulator system and the mechanism of the wearable haptic fingertip device.

[1]Chair of Information-oriented Control, Technische Universität München, Munich, Germany, e-mail: {selma.music, hirche}@tum.de

[2]Department of Information Engineering and Mathematics, University of Siena, Italy, e-mail: prattichizzo@ing.unisi.it

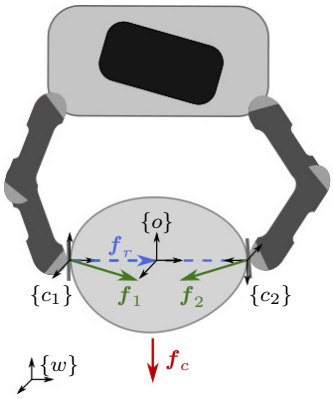

Fig. 1. Dual-manipulator system grasps a common object. The end-effector coordinate frames are $\{c_1\}$ and $\{c_2\}$, while the object frame is $\{o\}$. The world frame is denoted with $\{w\}$. Interaction forces, measured at the end-effectors, are denoted with $\boldsymbol{f}_1$ and $\boldsymbol{f}_2$. Their cooperative and relative force components are denoted with $\boldsymbol{f}_c$ and $\boldsymbol{f}_r$, respectively.

A. Cooperative dual-manipulator system

Fig. 1 depicts a dual-manipulator system grasping an object. The wrenches and velocities measured at the end-effectors, i.e. in $\{c_1\}$ and $\{c_2\}$ frames, are denoted with the vectors $\boldsymbol{h} = [\boldsymbol{h}_1^\top \ \boldsymbol{h}_2^\top]^\top \in \mathcal{R}^{12}$ and $\boldsymbol{v} = [\boldsymbol{v}_1^\top \ \boldsymbol{v}_2^\top]^\top \in \mathcal{R}^{12}$, respectively. The wrench vector is composed of forces and moments $\boldsymbol{h}_i = [\boldsymbol{f}_i^\top \ \boldsymbol{m}_i^\top]^\top$. The wrench and the velocity of the object are denoted with the vectors $\boldsymbol{h}_o$ and $\boldsymbol{v}_o$, respectively. As proposed in [11] we perform a cooperative manipulation task along two constraints: *cooperative* and *relative*.

Cooperative constraint defines the object motion. The *cooperative force*, $\boldsymbol{f}_o$, accelerates the object and counterbalances the gravitational forces. It is also termed as a *load force* in literature. The constraint is determined by the grasp matrix, provided there are no relative motions between the end-effectors

$$\boldsymbol{v} = \underbrace{\begin{bmatrix} \boldsymbol{I}_3 & \boldsymbol{S}^\top(\boldsymbol{r}_1) \\ \boldsymbol{0}_3 & \boldsymbol{I}_3 \\ \boldsymbol{I}_3 & \boldsymbol{S}^\top(\boldsymbol{r}_2) \\ \boldsymbol{0}_3 & \boldsymbol{I}_3 \end{bmatrix}}_{\boldsymbol{G}^\top} \boldsymbol{v}_o, \tag{1}$$

where $\boldsymbol{r}_1$ and $\boldsymbol{r}_2$ are vectors determining the relative displacement between the object and the end-effectors' frames. Wrench applied to the object is

$$\boldsymbol{h}_o = \boldsymbol{G}\boldsymbol{h}. \tag{2}$$

Relative constraint defines the relative motion between the manipulators, necessary to grasp the object. Once the object is grasped, the relative motion between the manipulators generates an increase in the relative force which maintains the grasp. The corresponding relative force, $\boldsymbol{f}_r$, does not contribute to the motion of the object but only to the grasp maintenance, guaranteeing that the contact forces satisfy the contact and friction constraints. Relative force of the dual-manipulator system with collinear normal vectors to the object is also termed as a *grip force* in literature. The constraint is defined by the following matrix equation

$$\boldsymbol{v}_r = \underbrace{\begin{bmatrix} \boldsymbol{I}_3 & \boldsymbol{S}(\boldsymbol{r}_{1,2}) & -\boldsymbol{I}_3 & \boldsymbol{0}_3 \\ \boldsymbol{0}_3 & \boldsymbol{I}_3 & \boldsymbol{0}_3 & -\boldsymbol{I}_3 \end{bmatrix}}_{\boldsymbol{A}} \boldsymbol{v}, \tag{3}$$

where $\boldsymbol{r}_{1,2}$ is the vector determining the relative displacement between the end-effectors and $\boldsymbol{v}_r$ is the relative velocity between the end-effectors. Relative force is defined as

$$\boldsymbol{f}_r = \boldsymbol{A}^{\#\top}\boldsymbol{h}$$

where $\boldsymbol{A}^{\#\top}$ is a pseudoinverse matrix.

In order to achieve desired performance of cooperative and relative behavior we use position-based impedance controllers. The desired cooperative and relative error dynamics are set as

$$\begin{aligned} &\boldsymbol{M}_o(\dot{\boldsymbol{v}}_o - \dot{\boldsymbol{v}}_o^d) + \boldsymbol{D}_o(\boldsymbol{v}_o^d - \boldsymbol{v}_o) + \boldsymbol{h}_o^K(\boldsymbol{x}_o^d, \boldsymbol{x}_o) = \boldsymbol{h}_o^m \\ &\boldsymbol{D}_r(\boldsymbol{v}_r^d - \boldsymbol{v}_r) + \boldsymbol{h}_r^K(\boldsymbol{x}_r^d, \boldsymbol{x}_r) = \boldsymbol{h}_r^m, \end{aligned} \tag{4}$$

where $\boldsymbol{M_o}$ is the desired cooperative inertia matrix, while $\boldsymbol{D}_o = \text{blockdiag}[d_{o,t}\boldsymbol{I}_3, d_{o,r}\boldsymbol{I}_3]$ and $\boldsymbol{D}_r = \text{blockdiag}[d_{r,t}\boldsymbol{I}_3, d_{r,r}\boldsymbol{I}_3]$ are the desired damping matrices, and the desired stiffnesses are defined as in [12]. Measured object and relative wrenches are $\boldsymbol{h}_o^m$ and $\boldsymbol{h}_r^m$, respectively. Further details on the general control architecture can be found in [11].

B. Human in the loop

The human operator commands desired motion trajectories to the dual manipulators and receives force feedback from their interaction with the object.

The relative velocity between the thumb and index fingers is the desired relative motion of the robots along the normals to the object surface at the contact points. Thumb and index fingers positions are denoted with $\boldsymbol{p}_1$ and $\boldsymbol{p}_2$ (see Fig. 2), respectively. The motion of the human hand, tracked with the frame $\{b\}$, is the desired motion of the object. The measured forces of the robot are fed back to the operators fingertips. The following holds

$$\begin{aligned} \boldsymbol{v}_r^d &= \dot{\boldsymbol{p}}_1 - \dot{\boldsymbol{p}}_2 \\ \boldsymbol{v}_c^d &= \boldsymbol{v}_b, \end{aligned}$$

where $\boldsymbol{v}_b$ is the velocity of the frame $\{b\}$.

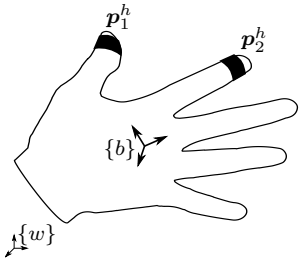

Fig. 2. The human operator guides the motion of the dual-manipulator system. Relative motion between the thumb and the index fingers generates relative motion between the two manipulators. The thumb and index finger positions are denoted with $\boldsymbol{p}_1^h$ ans $\boldsymbol{p}_2^h$, respectively. The motion of the human hand generates the motion of the object. Pose of the human hand is denoted with the frame $\{b\}$.

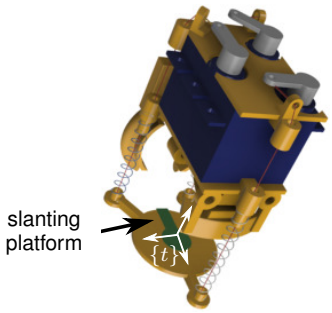

Fig. 3. Wearable haptic fingertip device. The slanting platform has 3 degrees of freedom: displacement, roll, and pitch. The local frame of the device is set in the middle of the platform and is denoted with $\{t\}$.

Wearable haptic device: The haptic device is illustrated in Fig. 3. Three motors control the length of the three tensors which are connected to the vertices of the slanting platform. The tensors pull the three vertices of the platform independently which results in 3 degrees of freedom of the platform: *roll* (α), *pitch* (β), and *displacement* (d). The slanting platform is located under the finger pulp of the user. The initial position of the platform is held by three springs. Operating principles of the fingertip device are detailed in [7], [9], and [13].

III. USER STUDY

In this section we describe the experimental setup, the conducted task, the user study design, and the obtained results.

A. Experimental setup

The experimental setup is presented in Fig. 4. Two KUKA LWR4+ manipulators are mounted on a common platform which is static for the purposes of this study. A box with 1 kg is the manipulated object. The system setup is rotated 90° w.r.t. the orientation of the subject's hand in $\{w\}$, shown in Fig. 5. In this way one of the end-effectors, as depicted in Fig. 4, is always occluded by the object and the operator cannot see it. Only translational degrees of freedom of the dual manipulator in the task space are activated, i.e. the rotations of the system cannot be controlled by the operator. The object is tracked by a motion capture system. The force at the end-effectors is estimated with the internal torque sensing of the manipulators and their known kinematic structure. The controller sampling frequency is 1 kHz, while the motion tracking system and the fingertip devices operate on 0.1 kHz. Due to the absence of the kinesthetic feedback, the low sampling frequency of the wearable haptic fingertip devices does not generate instability [7].

The human operator shares the workspace with the robots, i.e. they have the same reference frame $\{w\}$, and has direct visual feedback of the goal marks. The operator conducts the task while standing and can freely move in the workspace. Two fingertip devices are mounted on the human thumb and index fingers, as depicted in Fig. 5. Human hand, thumb, and index fingers are tracked with the motion tracking system.

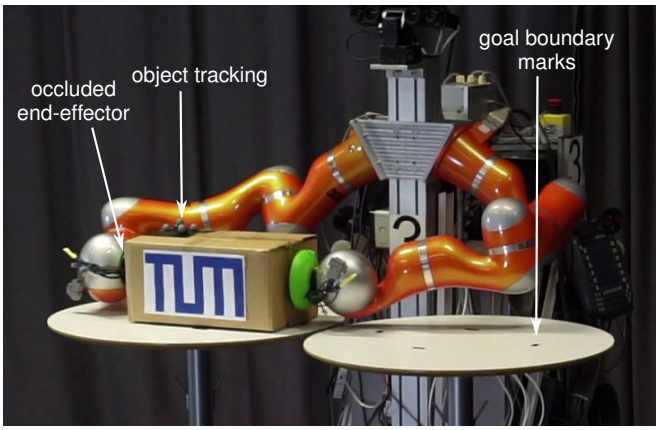

Fig. 4. Experimental setup. Two robot manipulators grasp and transport the object to the goal, denoted with the *boundary marks*. During the user study the field of view of the participants is rotated by 90°, i.e. one end-effector is always occluded.

The setup with the human in the loop has wireless and fully wearable capabilities by establishing communication between the human and the robot system via Raspberry Pi. However, to avoid potential effects of delay and package losses on the user study results, the feedback is delivered through a local network.

Task: The participants conduct a *pick-and-place* task. In particular, it is required to guide the robots to grasp the object by commanding the relative motion. Afterwards, the operator needs to command the manipulators to apply sufficient amount of relative force to overcome gravitational forces during the object lifting. This is achieved through the continued relative motion between the thumb and index fingers. The object is assumed to be rigid, i.e. the commanded motion results in the relative force build up between the manipulators. Desired object motion is commanded by the motion of the operator's hand. During the object transportation the operator needs to simultaneously control relative forces to avoid drops and slips. Boundaries of two goal positions are marked on two tables. In Fig. 4 only the markings for the second goal are visible since the object is already located on the first goal. The participants are asked to grasp the object from the start position (goal 1), transport it to the goal 2, and release the object when they consider they achieved a satisfactory precision by increasing the distance between the thumb and index fingers. This ends one trial. In the second trial the procedure is the same but the object is transported from the goal 2 to the goal 1.

Independent variables: Three independent conditions are types of force feedback received through the haptic devices:

1) *Visual feedback (VF)*: The operator receives only direct visual feedback, i.e. the platforms of the devices are at initial positions and do not exert pressure on the fingertips. Therefore, feedback forces on the thumb and index fingers in frame $\{t\}$are ${}^{t}f_t = {}^{t}f_i = 0$ N.
2) *Relative force feedback (RVF)*: The operator receives direct visual feedback and feedback of the relative force applied by the manipulators to the object. The

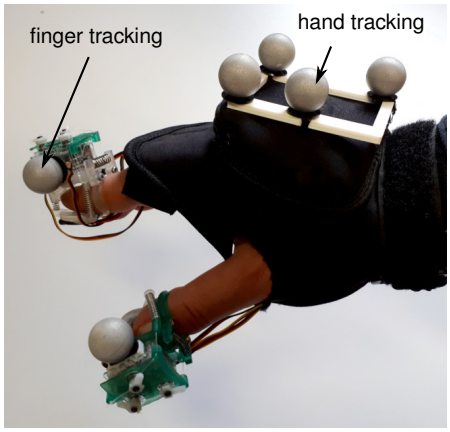

Fig. 5. Two fingertip wearable haptic devices are mounted on the subjects' thumb and index fingers. Hand, thumb, and index fingers are tracked with the mounted passive markers and a motion capture system.

TABLE I
INDEPENDENT CONDITIONS

1	VF	visual
2	RVF	relative + visual
3	MVF	measured + visual

rotational degrees of freedom of the haptic devices are not activated. Therefore, the displacement degree of freedom of the devices exerts normal forces on the operator fingers. In particular

$$ {}^t f_t = {}^t f_i = s_h {}^t f_r / 2, $$

where $s_h = \frac{4.7}{30}$ is a scaling factor, ${}^t f_t$ and ${}^t f_i$ are feedback forces in the fingertip frame on the thumb and the index fingers, respectively. The resulting displacements are

$$ {}^t d_t = k_t {}^t f_t \quad \text{and} \quad {}^t d_i = k_t {}^t f_i, \tag{5} $$

with the constant fingertip compliance parameter $k_t = 2$ mm/N [14].

3) *Total measured interaction force (MVF)*: The operator receives direct visual feedback and feedback about both the total measured interaction forces. The rotational degrees of freedom of the devices are activated. 3 DoFs of the thumb device display forces measured at the end-effector 1, while the index device displays forces measured at the end-effector 2

$$ \begin{aligned} &\alpha = \text{atan}\left(\frac{{}^t f_x^m}{{}^t f_z^m}\right), \ \beta = \text{atan}\left(\frac{{}^t f_y^m}{{}^t f_z^m}\right), \\ &d = k_t s_h \sqrt{\left({}^t \boldsymbol{f}^m\right)^\top {}^t \boldsymbol{f}^m}. \end{aligned} \tag{6} $$

where α and β provide shear forces at the contact points, while d displays the total force intensity.

The list of the independent conditions and their abbreviations are summarized in Table I.

Hypothesis: Force feedback types (RVF and MVF) outperform VF feedback type.

Dependent variables: In order to evaluate the performance of the four feedback conditions we analyze following dependent variables

1) mean relative force, $\bar{f}_r$,
2) maximum relative force during the lifting stage, f_r^{max},
3) power-based effort necessary to execute the task

$$ P = \boldsymbol{f}^\top \boldsymbol{v}, $$

4) total energy used to execute the task

$$ E = \int_0^T \boldsymbol{f}^\top \boldsymbol{v} \, \mathrm{d}t, $$

where T is trial duration, and
5) number of drops and slips.

Subjects: Sixteen healthy subjects participated in the user study. A *between-subjects (repeated-measures)* study is conducted, i.e. each subject performed the task under each independent condition. Each condition is performed 10 times. In order to avoid bias towards certain independent conditions, the order in which the conditions are performed is random for each subject.

B. Results

Fig. 6 shows the mean and standard deviation for relative (grip) and cooperative (load) force for all feedback conditions, normalized to $t = 1$ s. It can be observed that the lowest measured relative force is achieved with RVF condition. The load force is similar for all conditions. Fig. 7 shows that the ratio of the relative and cooperative forces is consistently the lowest for RVF condition. The ratio for MVF condition is lower than VF condition during the lifting stage. However, during the transportation stage the ratios for VF and MVF conditions are very similar. This indicates that MVF condition is not very beneficial form of haptic feedback during object motion. The reason may be that the displacement degree of freedom of the haptic device is overloaded with both relative and cooperative forces, which may generate difficulties in discriminating the type of force sensed at the fingertips.

Error measurements caused by the loss of hand tracking were excluded. There were 11% of such measurements that were linearly interpolated. The dependent variables are computed from the obtained data, filtered with a low-pass frequency filter with 6 Hz cut-off frequency. Statistical analysis is conducted using a *repeated-measures analysis of variance (rANOVA)*. A post-hoc multicomparison analysis is conducted using *Tukey-Kramer* method. *Mauchly's test of sphericity* revealed that all dependent variables violate the sphericity condition. Therefore, modification to the degrees of freedom is performed using *Greenhouse-Geiger* correction. In the remainder of this subsection we present the results of the statistical analysis. The significant differences between the conditions are denoted with $\star$ if $p < .05$, $\star\star$ if $p < .01$, $\star\star\star$ if $p < .001$, and $\star\star\star\star$ if $p < .0001$. Exact pairwise comparison p values are listed in Table II.

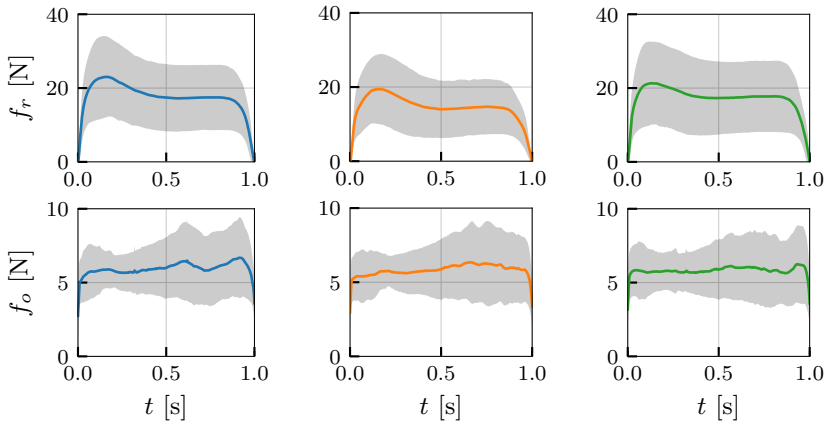

(a) VF (b) RVF (c) MVF

Fig. 6. Relative and cooperative force mean and standard deviation. With RVF feedback condition the lowest relative force is applied on the object.

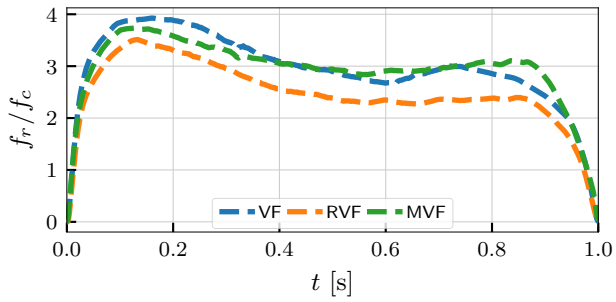

Fig. 7. Ratio between relative (grip) force and cooperative (load) force.

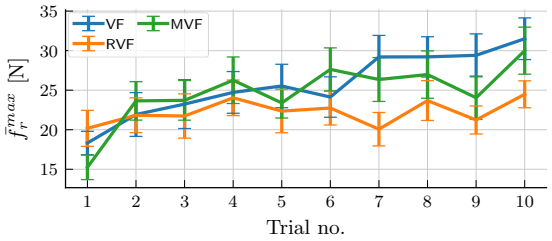

Fig. 9. Maximum measured relative force per 10 trials and across all subjects.

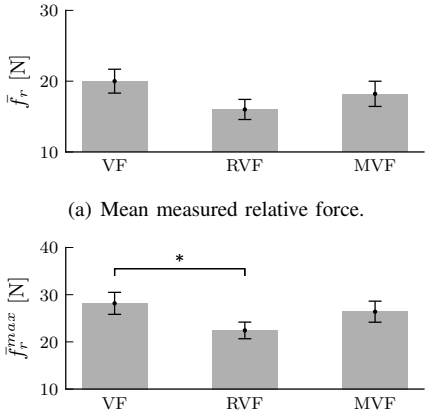

(a) Mean measured relative force.

(b) Maximum measured lift relative force.

Fig. 8. Bar plots of the average values of relevant performance measures across last five trials and all subjects. The vertical bars in the plots are standard errors (SEs).

1) Mean relative force and maximum lift relative force: Bar plots of five last trials for the mean relative force and maximum relative force during the lifting stage are depicted in Fig. 8(a) and Fig. 8(b), respectively. Drops were excluded from the analysis to avoid their effect on reducing the overall mean. No outliers were detected for the mean relative force measure, while 1% of the total measurements were outliers in maximum relative force measure. The statistical test did not reveal significant difference between the feedback conditions for mean relative force measure ($F(2, 30) = 2.9964, p = 0.068$). However, significant difference was revealed for maximum relative force measure ($F(2, 30) = 3.4413, p = 0.47$). In both cases, the measured force is the lowest for RVF condition. Multiple comparison revealed significant difference between VF and RVF conditions for maximum lift relative force measure.

Fig. 9 depicts maximum relative force across 10 trials for all feedback conditions. The relative force is consistently the lowest and kept constant for RVF feedback condition.

2) Total effort and energy: Bar plots for the total effort and energy are depicted in Fig. 10(a) and Fig. 10(b), respectively. For the effort dependent measure, outliers 4% of data were detected as outliers. Statistical analysis revealed significant differences between the feedback conditions ($F(2, 30) = 11.832, p = 0.00017$) for the effort measure but revealed no significant differences between conditions for the total energy measure ($F(2, 30) = 2.3744, p = 0.11$) for the power and the energy dependent measures, respectively. Both the effort and the energy are the lowest for RVF condition. Furthermore, the effort for RVF condition is significantly different from VF condition. This indicates the importance of force feedback in reducing the effort of task execution. Fig. 11 shows that for RVF condition the energy is the lowest for RVF and that it is approximately constant across all trials. For VF condition the total energy increases with the number of trials indicating fatigue of participants.

TABLE II

MULTIPLE COMPARISON p VALUES OBTAINED WITH BONFERRONI METHOD

Dependent variables	VF vs. RVF	VF vs. MVF	RVF vs. MVF
Mean rel. force, f_r	0.07	0.44	0.44
Max. rel. force, f_r^{max}	**0.04**	0.6	0.2
Effort, P	**0.0007**	**0.03**	0.13
Energy, E	0.1	0.59	0.5

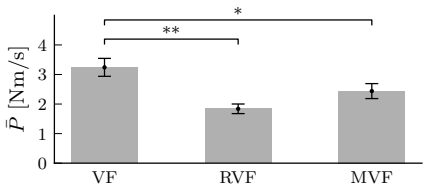

(a) Total effort.

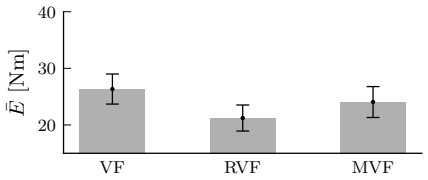

(b) Total energy.

Fig. 10. Bar plots of the average values of relevant performance measures across last five trials and all subjects. The vertical bars in the plots are standard errors (SEs).

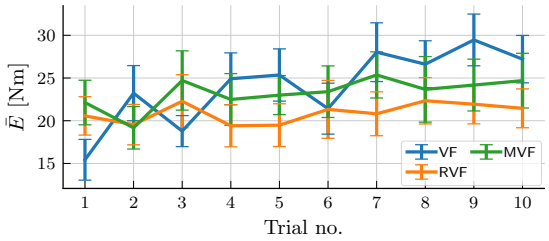

Fig. 11. Mean energy per 10 trials and across all subjects. The energy needed to conduct the task is consistently the lowest for RVF.

3) Drops and slips: Fig. 12 shows a cumulative bar plot with the total number of drops and slips across trials for each condition. The highest number of drops is detected for VF condition, while the lowest (only one drop) for MVF condition, indicating that the rotational degrees of freedom are beneficial in reducing drops and slips. The statistical analysis did not reveal significant difference between conditions. However, based on the occurrence of drops and slips per trials it can be concluded that for VF condition the drops and slips are the most frequent in earlier trials (1-4), but their frequency reduces in later trials as the applied relative force increases. Drops are more frequent in the later trials in RVF condition which may be an indication of fatigue.

IV. DISCUSSION

The results of the statistical analysis show that wearable haptic devices, provided with dynamic force feedback, improve the performance for cooperative manipulation tasks. For all analyzed dependent variables the condition RVF gives

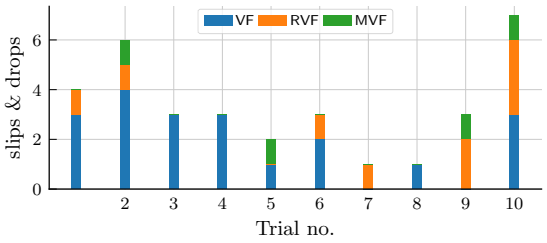

Fig. 12. Cumulative bar plot of the total number of drops and slips per 10 trials. The highest number of drops and slips is detected for VF condition. The lowest number of drops and slips is detected for MVF condition.

the best results which are significantly different in therms of maximum relative force applied, as well as for the total effort needed to conduct the task. This result indicates that displaying relative (grip) force through the displacement DoF of the fingertip devices is essential for cooperative manipulation tasks.

We assumed the same conclusion would hold for MVF condition. However, the results did not fully confirm our hypothesis. During the object transportation the mean relative force for VF and MVF is almost the same. This is not expected and may be influenced by the overload of force components on the displacement degree of freedom of the devices. In particular, the participants may be unable to discriminate between relative and cooperative effects if they are superimposed on a single degree of freedom. However, MVF condition significantly reduces the effort of conducting the task when compared to VF condition. It also reduces the number of drops and slips. This indicates the importance of using the rotational degrees of freedom of the fingertip haptic device to convey information about slips.

V. CONCLUSIONS

In this paper we present the results of a user study conducted with wearable haptic fingertip devices and a dual manipulation setup. We show that the haptic feedback indeed improves the task performance. In particular, the devices are suitable to convey information about relative (grip) force. The feedback about the measured forces at the contact points did not convey equally good results, even though its difference from purely visual feedback (VF) is significant in terms of total effort needed to conduct the task. The number of drops and slips is by far the lowest for MVF type of feedback indicating that it is possible to perceive slips through rotational degrees of freedom conveying shear forces. However, the results for this type of feedback are

still not conclusive and a simplified feedback of relative forces through the use of the displacement degree of freedom conveyed the best results.

ACKNOWLEDGMENT

The authors would like to thank Pablo Budde gen. Dohmann for his help with data acquisition. The work is partly funded from DFG-NSFC project "COVEMAS - Control and Optimization for Event-triggered Networked Autonomous Multi-agent Systems"

REFERENCES

[1] A. Mörtl, M. Lawitzky, A. Kucukyilmaz, M. Sezgin, C. Basdogan, and S. Hirche, "The role of roles: Physical cooperation between humans and robots," *The International Journal of Robotics Research*, vol. 31, no. 13, pp. 1656–1674, 2012. [Online]. Available: https://doi.org/10.1177/0278364912455366

[2] S. Hirche and M. Buss, "Human-oriented control for haptic teleoperation," *Proceedings of the IEEE*, vol. 100, no. 3, pp. 623–647, March 2012.

[3] T. Hulin, K. Hertkorn, P. Kremer, S. Schtzle, J. Artigas, M. Sagardia, F. Zacharias, and C. Preusche, "The dlr bimanual haptic device with optimized workspace," in *2011 IEEE International Conference on Robotics and Automation*, May 2011, pp. 3441–3442.

[4] T. H. Massie, J. K. Salisbury, *et al.*, "The phantom haptic interface: A device for probing virtual objects," in *Proceedings of the ASME winter annual meeting, symposium on haptic interfaces for virtual environment and teleoperator systems*, vol. 55, no. 1. Citeseer, 1994, pp. 295–300.

[5] J. C. Perry, J. Rosen, and S. Burns, "Upper-limb powered exoskeleton design," *IEEE/ASME Transactions on Mechatronics*, vol. 12, no. 4, pp. 408–417, Aug 2007.

[6] D. Prattichizzo, C. Pacchierotti, and G. Rosati, "Cutaneous force feedback as a sensory subtraction technique in haptics," *IEEE Transactions on Haptics*, vol. 5, no. 4, pp. 289–300, Fourth 2012.

[7] C. Pacchierotti, L. Meli, F. Chinello, M. Malvezzi, and D. Prattichizzo, "Cutaneous haptic feedback to ensure the stability of robotic teleoperation systems," *The International Journal of Robotics Research*, vol. 34, no. 14, pp. 1773–1787, 2015. [Online]. Available: https://doi.org/10.1177/0278364915603135

[8] S. Music, O. Khatib, and S. Hirche, "Shared control for robot-team teleoperation," in *2018 IEEE/RSJ International Conference on Intelligent Robots and Systems, Workshop on "Haptic-enabled shared control of robotic systems: a compromise between teleoperation and autonomy"*, Madrid, Spain, 2018.

[9] F. Chinello, M. Malvezzi, C. Pacchierotti, and D. Prattichizzo, "Design and development of a 3rrs wearable fingertip cutaneous device," in *2015 IEEE International Conference on Advanced Intelligent Mechatronics (AIM)*, July 2015, pp. 293–298.

[10] M. Gabardi, M. Solazzi, D. Leonardis, and A. Frisoli, "A new wearable fingertip haptic interface for the rendering of virtual shapes and surface features," in *2016 IEEE Haptics Symposium (HAPTICS)*, April 2016, pp. 140–146.

[11] S. Music, G. Salvietti, P. Budde genannt Dohmann, F. Chinello, D. Prattichizzo, and S. Hirche, "Human-robot team interaction through wearable haptics for cooperative manipulation," *IEEE Transactions on Haptics*, pp. 1–1, 2019.

[12] F. Caccavale, P. Chiacchio, A. Marino, and L. Villani, "Six-dof impedance control of dual-arm cooperative manipulators," *IEEE/ASME Transactions on Mechatronics*, vol. 13, no. 5, pp. 576–586, Oct 2008.

[13] D. Prattichizzo, F. Chinello, C. Pacchierotti, and M. Malvezzi, "Towards wearability in fingertip haptics: A 3-DoF wearable device for cutaneous force feedback," *IEEE Transactions on Haptics*, vol. 6, no. 4, pp. 506–516, Oct 2013.

[14] K.-H. Park, B.-H. Kim, and S. Hirai, "Development of a soft-fingertip and its modeling based on force distribution," in *IEEE International Conference on Robotics and Automation*, vol. 3, 2003, pp. 3169–3174.